Eur Biophys J (2010) 39:1089–1095
DOI 10.1007/s00249-009-0518-x

ORIGINAL PAPER

Modulating the activity of the channel-forming segment of Vpr protein from HIV-1

Chin-Pei Chen · Clemens Kremer · Peter Henklein · Ulrich Schubert · Rainer H. A. Fink · Wolfgang B. Fischer

Received: 26 February 2009 / Revised: 27 June 2009 / Accepted: 29 June 2009 / Published online: 24 July 2009

Abstract Viral protein of regulation (Vpr) encoded by human immunodeficiency virus type 1 (HIV-1) is a short auxiliary protein that is 96 amino acids in length. During the viral life cycle, Vpr is released into the blood serum and is able to enter cellular membranes of noninfected cells. In this study a short peptide, $Vpr_{55–83}$, was shown to exhibit ion-channel-like activity when reconstituted into (1) planar lipid bilayers and (2) lipid bilayers held at the tip of a glass pipette. The two set-ups led to differences in the oligomerization state of the peptide, which was reflected in differences in the conductance levels. Experiments under applied hydrostatic pressure affect the dynamics of the protein within the membrane.

Keywords Vpr · HIV-1 · Planar lipid bilayers · Membrane protein

Viral membrane proteins, Heidelberg, December 2008.

C.-P. Chen · W. B. Fischer (✉)
Institute of Biophotonics,
School of Biomedical Science and Engineering,
National Yang Ming University, Taipei 112, Taiwan
e-mail: wfischer@ym.edu.tw

C. Kremer · R. H. A. Fink
Institute of Physiology and Pathophysiology,
University of Heidelberg, 69120 Heidelberg, Germany

P. Henklein
Institute of Biochemistry, Charité,
Universitätsmedizin Berlin, 10117 Berlin, Germany

U. Schubert
Institute of Clinical and Molecular Virology,
University of Erlangen-Nürnberg, 91054 Erlangen, Germany

Introduction

Viral protein of regulation (Vpr) is a 96-amino-acid protein (∼14 kDa) that belongs to a set of regulatory or auxiliary proteins encoded by HIV-1, including Tat, Rev, Vpu, Nef, and Vif (Wong-Staal et al. 1987; Bukrinsky and Adzhubei 1999). None of these auxiliary proteins is essential for viral replication in tissue culture, but they are important for viral replication in experimentally infected rhesus macaques (Lang et al. 1993) and highly conserved in human and primate immunodeficiency viruses.

Vpr has been found to induce a series of effects in nondividing host cells such as support of the viral preintegration process across the nuclear pore (Heinzinger et al. 1994; Popov et al. 1998), stimulation of gene expression (Cohen et al. 1990b; Stark and Hay 1998), induction of G_2 cell-cycle arrest (Jowett et al. 1995; Mahalingam et al. 1995; Rogel et al. 1995), and modulation of HIV-induced apoptosis (Ayyavoo et al. 1997; Stewart et al. 1997). Vpr is found in the virion (Cohen et al. 1990a; Müller et al. 2000) and in the blood and cerebral fluid of HIV-1 carriers (Levy et al. 1994). When administered extracellularly, Vpr can penetrate the plasma membrane and therefore access intracellular compartments (Arunagiri et al. 1997; Kichler et al. 2000) such as the mitochondria and nucleus. The route of entering the mitochondria is still controversial but may involve the formation of lipid pores or interaction with other mitochondrial factors such as voltage-dependent anion channels (VDACs) and the adenine nucleotide translocator (ANT) (Basañez and Zimmerberg 2001).

Ion current passing through peptide-generated pores is commonly measured under voltage clamp conditions using a "bilayer" or "black lipid membrane" technique (Montal and Müller 1972). With this technique it has been shown that Vpr reconstituted into artificial membranes induces the

formation of channels or pores either as a full-length protein (Piller et al. 1996) or from specific Vpr-derived peptides (Jacotot et al. 2001).

Vpr has been shown to oligomerize into dimers in aqueous trifluoroethanol (TFE) and oligomerizes to higher aggregates in aqueous solution (Henklein et al. 2000). In this study we use the synthetic peptide $Vpr_{55–83}$, which is believed to be helical, as shown by NMR spectroscopy of full-length Vpr in 30% trifluoroethanol (Wecker et al. 2002). A peptide corresponding to $Vpr_{52–96}$ has also exhibited channel activity in artificial bilayers (Jacotot et al. 2001).

The bilayer technique has also been used to assess channel activity of a variety of other viral membrane proteins and peptides (reviewed in Montal 2003; Fischer and Krüger 2009). Nonviral peptides have also been tested for their capability to form channels, for example the classical examples of alamethicin and gramicidin (Hanke and Boheim 1980; Woolley and Wallace 1992) or artificial peptides such as $LSSLLSL_n$ ($n = 1, 2$) (Akerfeldt et al. 1993).

For the present study, we used the bilayer technique in two modifications in order to be able to impose different mechanical force fields on the membrane and the inserted peptide formation. In one modification, the artificial membrane covers the aperture of the tip of a patch pipette ("tip-dip method") (Szabo et al. 1969; Coronado and Latorre 1983; Hanke et al. 1984). In this modification, gravitational forces act perpendicularly on the membrane due to the horizontal mounting. However, comparably stronger forces are generated by surface charges of the glass walls and the membrane (Fig. 4b). In the other modification, the bilayer is generated by raising two lipid monolayers, which cover an aqueous reservoir on the two sides of an aperture (Montal and Müller 1972). Gravitational forces act mainly in the plane of the membrane (BLM) due to the vertical mounting of the membrane. In this set-up, the membrane may also be painted across the aperture (hereafter referred to as the "painting technique"). Reconstitution of the proteins or peptides using this set-up can follow a series of protocols such as flashing the relevant peptide/protein against the membrane, "pre-incubating" the lipids with the peptide/protein (Mehnert et al. 2007), or using vesicle fusion to import the protein/peptide into the artificial membrane.

In this study, the two set-ups (tip-dip and painting) and their effects on the activity of $Vpr_{55–83}$ are assessed. So far researchers have usually used only one of the two set-ups and methods to investigate their protein/peptide of choice. Gramicidin is one of the rare occasions where both techniques were used by the same group (Matsuno et al. 2004). With the tip-dip method, the curvature of the membrane can be changed with application of hydrostatic pressure through the pipette. Based on the data, the in vivo mode of action of Vpr can be assessed when perturbing the lipid membrane after diffusion through the blood sera.

Materials and methods

Peptide synthesis

The sequence-based protein partner search (SPPS) for $Vpr_{55–83}$ (AGVEAIIRIL$_{10}$ QQLLFIHFRI$_{20}$ GCRHSRIGV–$CONH_2$) (Henklein et al. 2000) was performed on an ABI 433A automated peptide synthesizer equipped with a UV-detector from Applied Biosystems on a 0.1 mM scale using the Fmoc/*tert*-butyl strategy. The following side-chain-protecting groups were used during the automated synthesis: 2,2,4,6,7-pentamethyl-dihydro-benzofuran-5-sulfonyl (Arg), *tert*-butyl ether (Ser), *tert*-butyl ester.

After the synthesis, the three peptides were cleaved from the resin with trifluoroacetic acid/water/triisopropylsilane (95:3:2 v/v/v) for 3.5 h at room temperature. After evaporation of the cleavage solution and addition of ice-cold diethyl ether, the crude product was obtained as a white precipitate. The crude peptides were purified by reverse-phase HPLC (RP-HPLC) on a Shimadzu LC8 preparative HPLC using a Zorbax SB C18 column (21.2 × 250 mm, 7 µm, Agilent) with a linear gradient of 39% A to 60% B in 50 min (A: 2,500 ml water, 5 ml TFA; B: 2,000 ml acetonitrile, 500 ml water, 5 ml TFA) at a flow rate of 10 ml/min with spectrometric monitoring at $\lambda = 220$ nm to give the final pure products. The purity of the peptides was checked by RP-HPLC (Shimadzu LC10) on a Nucleosil 300 C18 (4.6 × 125 mm, 5 µm) with a linear gradient of 10% A to 100% B over 45 min. ESI-MS and MALDI-TOF-MS confirmed the correct mass of the product.

Channel recordings

All chemicals used in the experiments, such as potassium chloride (KCl), trifluoroethanol (TFE), chloroform, *n*-hexane, and HEPES were obtained from Sigma-Aldrich (USA) and used without further purification. All of the reagents were dissolved in deionized water (resistivity of >16.8 $M\Omega\,cm^{-1}$) from an ultra-pure water system (Millipore, USA). The buffer solutions were filtered through 0.22-µm Milex-GS filters from Millipore prior to use. Synthetic lecithins 1-palmitoyl-2-oleoyl-*sn*-glycero-3-phosphoethanolamine (POPE) and 1,2-dioleoyl-*sn*-glycero-3-phosphocholine (DOPC) (purity 99%) were purchased from Avanti Polar Lipids (USA).

A lipid mixture of POPE and DOPC (1:4 weight ratio, total 5 mg/ml) dissolved in *n*-hexane (1 mg/ml) was painted onto the aperture in the Delrin cup (diameter of aperture 150 µm) and dried under N_2. The two chambers of the Delrin cup were then filled with buffer solution (140 mM KCl, 5 mM K^+-HEPES, pH 7.0). The peptide was dissolved in TFE (1 mg/ml), mixed with a 1:4 mixture of POPE and DOPC (total 5 mg/ml) dissolved in chloroform, and dried

under N_2. The sample was then re-suspended in hexane leading to a final concentration of 1.0 mg/ml for lipid and 200 ng/ml for $Vpr_{55–83}$. With a paintbrush, the sample was transferred to the aperture of the Delrin cup covered by buffer (painting method). The two chambers were connected to ground (*trans*) and the input (*cis*) of an BC-535 amplifier (Warners Instruments, USA). The two chambers were connected via Ag/AgCl/agar bridges. Voltages were measured in the *cis*-chamber with respect to the grounded *trans*-chamber. Bilayer formation was monitored electrically from the amplitude of the current pulse generated by a voltage ramp (typically a capacity of about 0.6 μF/cm^2). The current response was recorded using a 1440A data acquisition system from Axon Instruments (USA). Data were filtered with a Bessel-8-pole low-pass-filter at 100 Hz.

Patch-clamp pipettes from borosilicate glass capillary were made using a microelectrode puller (Science Products, Hofheim, Germany), and the broken ends were fire-polished. Glass pipettes were filled with 140 mM KCl, 5 mM K^+-HEPES, pH 7.0, and the tip was immersed in a petri dish filled with the same solution. After immersion of the pipette, a mixture of lipid (1 mg/ml) and $Vpr_{55–83}$ (1 mg/ml) solution in *n*-hexane was added to run down the pipette shaft. Channel reconstitution into the lipid bilayer at the tip of the patch pipettes was achieved by lowering and raising the glass pipette above the solution level (tip-dip method). The solution was connected to ground (*trans*) and the pipette (*cis*) to a patch-clamp 200A amplifier (Axon Instruments). The *trans*-electrode was embedded in agar gel. Voltages were measured in the *cis*-chamber with respect to the grounded *trans*-chamber. Bilayer formation was monitored as the resistance (around 10 GΩ for a bilayer). The current response was recorded using an Axopatch 1D amplifier with a IHS-1 integrated headstage (Axon Instruments), and data were filtered with a Bessel-8-pole low-pass-filter at 100 Hz.

Data analysis

The conductance histograms were calculated from the superposition of individual conductance histograms, determined by the traces at the respective holding potentials. Each conductance histogram shows dwell-time-weighted Gaussian distribution functions for the opening events (Mehnert et al. 2008). The mean open time was calculated for each conductance state from cumulative dwell-time histograms fitted with an exponential decay function applying a steepest descent gradient method (Mehnert et al. 2007).

Results and discussion

A short segment of Vpr, $Vpr_{55–83}$, is investigated for its ability to form channels in planar lipid bilayers. Using the "painting" method, we obtain events (Fig. 1a) with conductance of 8 and 16 pS, with the latter more prominent (Fig. 1b). Using the "tip-dip" method, channel recordings (Fig. 2a) show events with conductance levels in the range of 50–80 pS (O_1) and 120–160 pS (O_2) (Fig. 2b). The first open level (O_1) can be resolved into a pattern with the most counts at 65 pS and fewer counts at 80 pS and 54 pS. This pattern is also reflected in the second open level (O_2) with the counts following the sequence 131 pS > 142/147 pS > 117 pS. At 167–172 pS, a set of two smaller conductance levels is resolved. A collection of opening events with 9 and 13 pS conductance levels is observed in bursts with open times less than 150 ms. To calculate the I/V curve using the tip-dip method, for each holding potential an averaged value for the two levels based on a single Gaussian fit (∼60 and 130 pS) is calculated. The I/V curve of the events indicates an Ohmic behavior for both techniques (Figs. 1c, 2c). The mean open time, τ_0, is also calculated as a mean value from all the events. τ_0 is voltage independent in the recordings using the tip-dip method and is found to be around 0.75 s (Fig. 3). Based on the limited number of events for the painting method, a result cannot be given. For positive holding potentials using the painting method, τ_0 is observed to be around 1.5 and 2.9 s at −60 mV. It is most likely that the mean open time is larger than reported for the tip-dip method and may be voltage dependent.

In all cases, the higher conductance levels are found to be twice as big as the values for the lower conductance levels. Therefore the lower levels can be seen as events from a "single" large assembly and the larger levels from an opening of another assembly. This is supported by the finding that the event patterns found with the tip-dip method are almost identical for both levels. Using the tip-dip method, conductance levels of 9 and 13 pS also arise, which should reflect the assembly reported for the painting method.

In another experiment, the effect of membrane curvature on the conductance levels of Vpr is investigated. Hydrostatic pressure is induced upon the membrane to generate a curvature. Without any pressure (p_0), conductance levels of 154 pS (main conductance level) and occasional short openings at 50 pS are observed (Figs. 2, 4a). Imposing positive pressure (+p), levels of 134 pS with short openings at 52 pS are found. Upon negative pressure (−p), the conductance levels are calculated to be 160 and 65 pS (short events). There is evidence that the τ_0 of the main conductance level at −p is lower ($\tau_0 = 0.54 \pm 0.1$ s) than at standard pressure p_0 ($\tau_0 = 0.91 \pm 0.1$ s). Upon +p, the mean open time ($\tau_0 = 0.87 \pm 0.1$ s) is similar to τ_0 at p_0. In the recording under −p, a flickering occurred. The flickering starts from the closed or any open state and can be envisaged as an effort of the assembly to reopen and conduct ions. Under standard conditions, it is anticipated that the

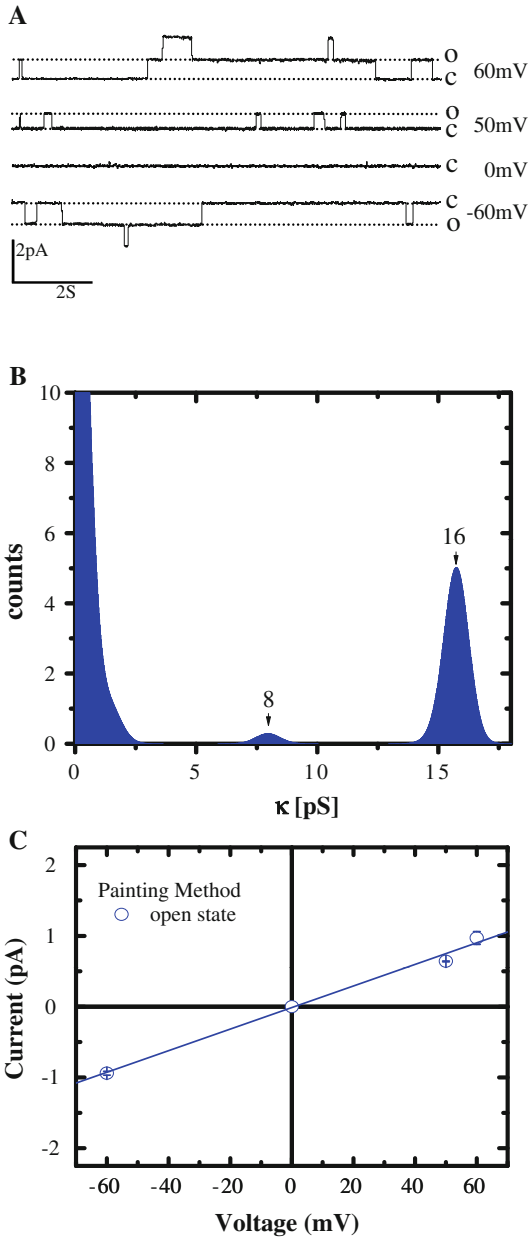

Fig. 1 Representative channel recordings from an experiment with synthetic $Vpr_{55–83}$ reconstituted into a lipid bilayer membrane composed of DOPC and POPE (weight ratio 4:1) on the Teflon Delrin Cup (painting method) (**a**). Currents are recorded in symmetric buffer conditions (140 mM KCl, 5 mM Hepes, pH 7.4 at room temperature). The *solid lines* labeled with *c* indicate the current of the closed state, while *o* indicates the opened state. All traces are filtered at 100 Hz with an 8-pole Bessel filter. Conductance histograms obtained from all traces are shown (**b**) and the respective current-voltage dependency of the data (**c**). Data are the standard error of mean (SEM, $n = 3$)

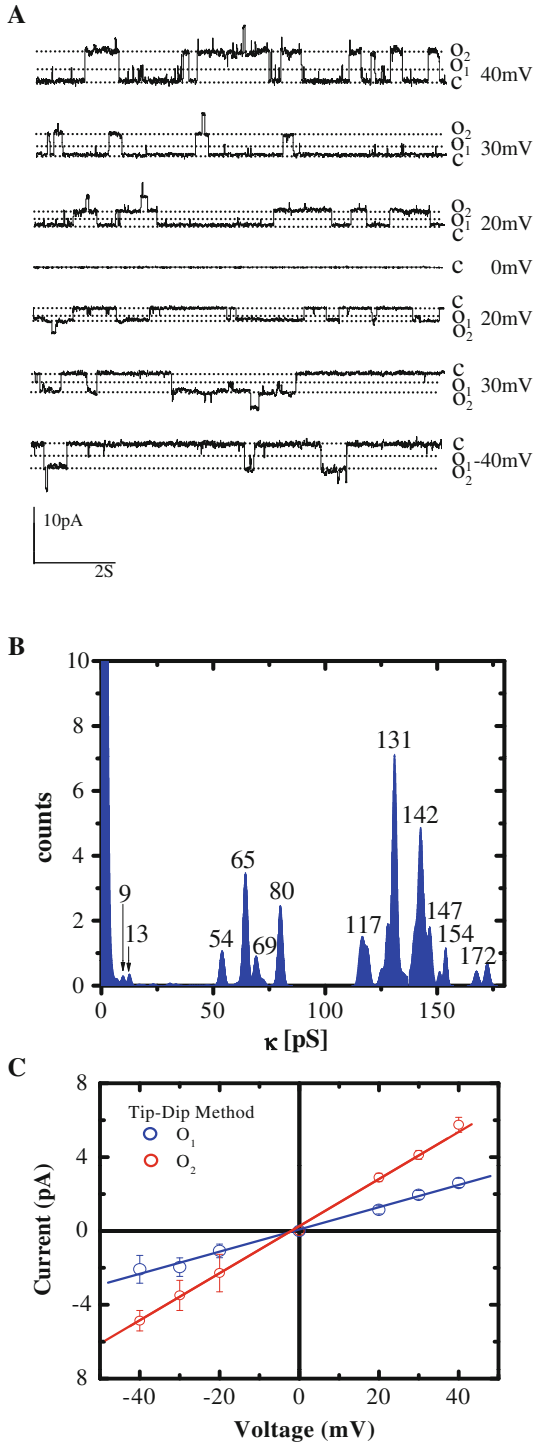

Fig. 2 Representative channel recordings from an experiment with synthetic $Vpr_{55–83}$ reconstituted into a lipid bilayer membrane composed of DOPC and POPE (weight ratio 4:1) at a glass pipette (**a**). Currents are recorded in symmetric buffer conditions (140 mM KCl, 5 mM Hepes, pH 7.4 at room temperature) (tip-dip method). The *solid lines* labeled with *c* indicate the current of the closed state, while *o* indicates the opened state. All traces are filtered at 100 Hz with an 8-pole Bessel filter. Conductance histograms obtained from all traces (**b**) and the respective current voltage dependency of the data (**c**). Data are the standard error of mean (SEM, $n = 3$)

membrane is slightly curved (Fig. 4b). Imposing a positive pressure may result in a flattening of the membrane (Fig. 4c), and under negative pressure an increase in curvature is anticipated (Fig. 4d). The rare short openings under standard conditions (p_0) can just be rare flickering events

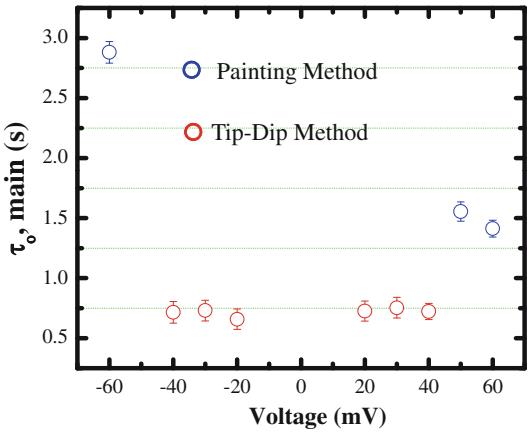

Fig. 3 Mean open time, τ_0, of the main conductance state of $Vpr_{55–83}$ channels as a function of the externally applied potential difference. The data are taken from the representative channels reported in Figs. 1 and 2. Data are the standard error of mean (SEM, $n = 3$)

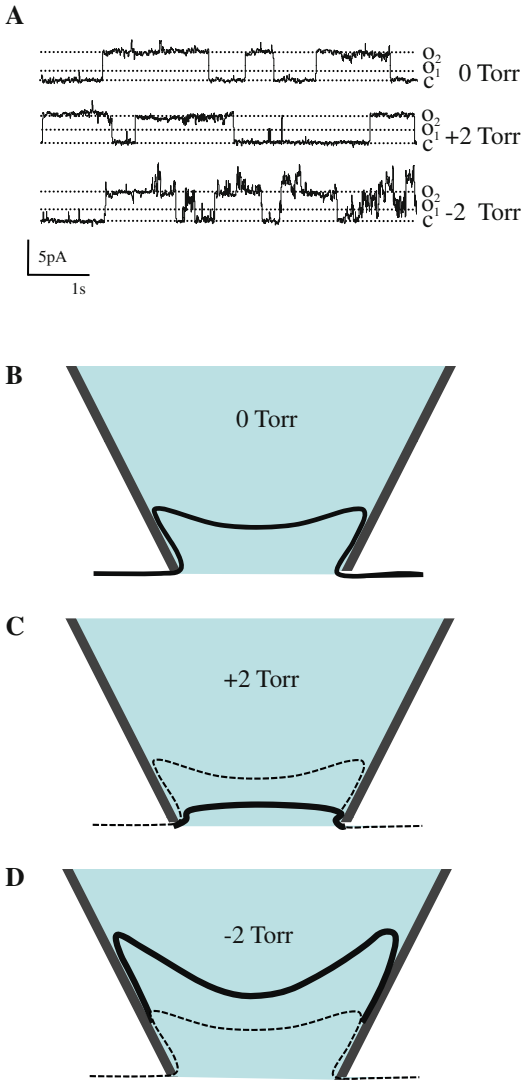

Fig. 4a–d Channel activity of $Vpr_{55–83}$ at a holding potential of +20 mV (140 mM KCl, 5 mM Hepes, pH 7.4 at room temperature) using the dip-tip method. The traces are recorded at 0 Torr (*upper trace*), +2 Torr (*middle trace*), and −2 Torr (*lower trace*) (**a**). Anticipated membrane curvatures are shown when the applied pressure is 0 Torr (**b**), +2 Torr (**c**), and −2 Torr (**d**). The anticipated membrane curvature at 0 Torr is shown as a dashed line in **c** and **d**. The *shaded area* indicates the buffer within the pipette. The pipette is shown in *grey* with its aperture pointing to the bottom of the figure

due to membrane undulation, which leads to local patches with increased curvatures. Upon increased membrane curvature ($-p$), these events occur more often and cause the flickering pattern.

Two explanations can be considered for the differences observed in conductance levels and kinetics: (1) lipid dynamics and (2) protein assembly, which may be affected differently by the mechanical force fields acting mainly laterally or perpendicularly on or in the membrane components under the various experimental conditions in our study.

The small aperture of the glass pipette (tip-dip method) can cause a bend in the bilayer due to electrostatic interactions between the glass wall and lipids (Fig. 4b). The electrostatic interaction induces a mechanical force field in the narrow geometry of the pipette tip, inducing membrane curvature (Honoré et al. 2006; Suchyna and Sachs 2007). The mechanical force field can affect the lateral diffusivity and dynamics of the lipids and the proteins with the consequence of altered protein mechanics (gating). Also the hydrostatic pressure induced by the difference in the height of the buffer levels in the pipette and the bath solution affects the membrane curvature. In the painting method setup, gravitational forces can lead to a thickening of the lipid annulus towards the "bottom" of the aperture and consequently to an altered lateral stress profile and lipid dynamics. Inducing an increase in membrane curvature as shown in this study indeed affects the kinetics and dynamics of the inserted peptide.

The difference in the conductance levels is also most likely due to the oligomerization state of the peptide. Due to the preparation protocol, the starting conditions for the Delrin cup are such that the peptide is dissolved in TFE and immediately immersed in lipids dissolved in chloroform. From previous studies in TFE-containing solvents, it can be extrapolated that a dimeric assembly seems to occur (Henklein et al. 2000). For the reconstitution protocol used for the tip-dip method, the peptide was dissolved in hexane and run down the pipette shaft. Possibly this protocol leads to an exposure of the peptide to an aqueous environment that enhances aggregation (Henklein et al. 2000) causing the higher conductance levels of 60 and 130 pS. The larger aggregates then have a lower mean open time. This value cannot be attributed to an event of an individual (in vivo) $Vpr_{55–83}$ bundle. It is instead the increase in membrane curvature that affects the dynamics of the assembly, and the

environment that affects the oligomerisation state. The lipid environment does not dilute the larger oligomers, once they have been formed, into smaller units.

Taking the dimer as the smallest unit of a functional Vpr, the number of peptides involved in any kind of near barrel-stave-like or toroidal assembly (Yang et al. 2001) should be a multiple of two. Increased membrane curvature seems to shorten the lifetime of the open state based on the altered lateral pressure profile of the membrane and increases the conductance levels. The observed flickering may be an indication that the closed state is not necessarily kinetically a more stable state than the open state. The results are another indication of the sensitivity of the pore-forming proteins to the lipid environment as mentioned in an earlier study (Mehnert et al. 2008).

Conclusions

In conclusion, our results confirm that the short segment of Vpr is responsible for channel activity in planar lipid bilayers with a conductance state of about 8–15 pS. It may be essential to leave Vpr in a lipidic environment during the preparation process in order to achieve the lowest conductance levels.

The mode of action of Vpr can be affected by membrane curvature and the exposure to different environments. Vpr may embed in the membrane as a larger assembly and be most effective (in an open state) in flat membrane patches rather than in highly curved areas of the membrane.

Acknowledgments WBF thanks the NYMU and the government of Taiwan for financial support (Aim of Excellence Program). This work was supported by the National Science Council of Taiwan (NSC) and a Taiwanese–German scholarship to C.C. C.C. also acknowledges a DAAD fellowship.

References

Akerfeldt KS, Lear JD, Wasserman ZR, Chung LA, DeGrado WF (1993) Synthetic peptides as models for ion channel proteins. Acc Chem Res 26:191–197

Arunagiri C, Macreadie I, Hewish D, Azadi A (1997) A C-terminal domain of HIV-1 accessory protein Vpr is involved in penetration, mitochondrial dysfunction and apoptosis of human CD4+ lymphocytes. Apoptosis 2:69–76

Ayyavoo V, Mahboubi A, Mahalingam S, Ramalingam R, Kudchodkar S, Williams WV, Green DR, Weiner DB (1997) HIV-1 Vpr suppresses immune activation and apoptosis through regulation of nuclear factor kB. Nat Med 3:1117–1123

Basañez G, Zimmerberg J (2001) HIV and apoptosis death and the mitochondrion. J Exp Med 193:F11–F14

Bukrinsky M, Adzhubei A (1999) Viral protein R of HIV-1. Rev Med Virol 9:39–49

Cohen EA, Dehni G, Sodroski JG, Haseltine WA (1990a) Human immunodeficiency virus Vpr product is a virion-associated regulatory protein. J Virol 64:3097–3099

Cohen EA, Terwilliger EF, Jalinoos Y, Proulx J, Sodroski JG, Haseltine WA (1990b) Identification of HIV-1 Vpr product and function. J Acquir Immune Defic Syndr 3:11–18

Coronado R, Latorre R (1983) Phospholipid bilayers made from monolayers on patch-clamp pipettes. Biophys J 43:231–236

Fischer WB, Krüger J (2009) Viral channel forming proteins. Int Rev Cell Mol Biol 275:35–63

Hanke W, Boheim G (1980) The lowest conductance state of the alamethicin pore. Biochim Biophys Acta 596:456–462

Hanke W, Methfessel C, Wilmsen U, Boheim G (1984) Ion channel reconstitution into lipid bilayer membranes on glass patch pipettes. Bioelectrochem Bioenerg 173:329–339

Heinzinger NK, Bukrinsky MI, Haggerty SA, Ragland AM, Kewalramani V, Lee MA, Gendelman HE, Ratner L, Stephenson M, Emerman M (1994) The Vpr protein of human immunodeficiency virus type 1 influences nuclear localization of viral nucleic acids in nondividing host cells. Proc Natl Acad Sci USA 91:7311–7315

Henklein P, Bruns K, Sherman MP, Tessmer U, Licha K, Kopp J, de Noronha CM, Greene WC, Wray V, Schubert U (2000) Functional and structural characterization of synthetic HIV-1 Vpr that transduces cells, localizes to the nucleus, and induces G2 cell cycle arrest. J Biol Chem 275:32016–33226

Honoré E, Patel AJ, Chemin J, Suchyna TM, Sachs F (2006) Desensitization of mechano-gated K_{2P} channels. Proc Natl Acad Sci USA 103:6859–6864

Jacotot E, Ferri KF, El Hamel C, Brenner C, Druillennec S, Hoebeke J, Rustin P, Metivier D, Lenoir C, Geuskens M, Vieira HL, Loeffler M, Belzacq AS, Briand JP, Zamzami N, Edelman L, Xie ZH, Reed JC, Roques BP, Kroemer G (2001) Control of mitochondrial membrane permeabilization by adenine nucleotide translocator interacting with HIV-1 viral protein rR and Bcl-2. J Exp Med 193:509–519

Jowett JBM, Planelles V, Poon B, Shah NP, Chen ML, Chen ISY (1995) The human immunodeficiency virus type 1 Vpr gene arrests infected T cells in the G2 + M phase of the cell cycle. J Virol 69:6304–6313

Kichler A, Pages JC, Leborgne C, Druillenec S, Lenoir C, Coulaud D, Delain E, Le Cam E, Roques BP, Danos O (2000) Efficient DNA transfection mediated by the C-terminal domain of human immunodeficiency virus type 1 viral protein R. J Virol 74:5424–5431

Lang SM, Weeger M, Stahl-Hennig C, Coulibaly C, Hunsmann G, Müller J, Müller-Hermelink H, Fuchs D, Wachter H, Daniel MM (1993) Importance of Vpr for infection of rhesus monkeys with simian immunodeficiency virus. J Virol 67:902–912

Levy DN, Refaeli Y, MacGregor BR, Weiner DB (1994) Serum Vpr regulates productive infection and latency of human immunodeficiency virus type 1. Proc Natl Acad Sci USA 91:10873–10877

Mahalingam S, Ayyavoo V, Patel M, Kieber-Emmons T, Weiner DB (1995) Nuclear import, virion incorporation, and cell cycle arrest/differentiation are mediated by distinct fucntional domains of the human immunodeficiency virus type 1 Vpr. J Virol 71:6339–6347

Matsuno Y, Osono C, Hirano A, Sugawara M (2004) Single-channel recordings of gramicidin at agarose-supported bilayer lipid membranes formed by the tip-dip and painting methods. Analyt Sci 20:1217–1221

Mehnert T, Lam YH, Judge PJ, Routh A, Fischer D, Watts A, Fischer WB (2007) Towards a mechanism of function of the viral ion channel Vpu from HIV-1. J Biomol Struct Dyn 24:589–596

Mehnert T, Routh A, Judge PJ, Lam YH, Fischer D, Watts A, Fischer WB (2008) Biophysical characterisation of Vpu from HIV-1 suggests a channel-pore dualism. Proteins 70:1488–1497

Montal M (2003) Structure-function correlates of Vpu, a membrane protein of HIV-1. FEBS Lett 552:47–53

Montal M, Müller P (1972) Formation of bimolecular membranes from lipid monolayers and a study of their electrical properties. Proc Natl Acad Sci USA 69:3561–3566

Müller B, Tessmer U, Schubert U, Kräusslich H-G (2000) Human immunodeficiency virus type 1 Vpr protein is incorporated into the virion in significantly smaller amounts than Gag and is phosphorylated in infected cells. J Virol 74:9727–9731

Piller SC, Ewart GD, Premkumar A, Cox GB, Gage PW (1996) Vpr protein of human immunodeficiency virus type 1 forms cation-selective channels in planar lipid bilayers. Proc Natl Acad Sci USA 93:111–115

Popov S, Rexach M, Zybarth G, Reiling V, Lee MA, Ratner L, LM A, Moore MS, Blodel G, Bukrinsky M (1998) Viral protein R regulates nuclear import of the HIV-1 preintegration complex. EMBO J 17:909–917

Rogel ME, Wu LI, Emerman M (1995) The human immunodeficiency virus type 1 Vpr gene prevents cell proliferation during chronic infection. J Virol 69:882–888

Stark LA, Hay RT (1998) Human immunodeficiency virus type 1 (HIV-1) viral protein R (Vpr) interacts with Lys-tRNA synthetase: implications for priming of HIV-1 reverse transcription. J Virol 72:3037–3044

Stewart SA, Poon B, Jowett JB, Chen IS (1997) Human immunodeficiency virus type 1 Vpr induces apoptosis following cell cycle arrest. J Virol 71:5579–5592

Suchyna TM, Sachs F (2007) Mechanosensitive channel properties and membrane mechanics in mouse dystrophic myotubes. J Physiol 581:369–387

Szabo G, Eisenman G, Ciani S (1969) The effects of the macrotetralide actin antibiotics on the electrical properties of phospholipid bilayer membranes. J Membr Biol 1:346–382

Wecker K, Morellet N, Bouaziz S, Roques BP (2002) NMR structure of the HIV-1 regulatory protein Vpr in H2O/trifluoroethanol. Comparison with the Vpr N-terminal (1–51) and C-terminal (52–96) domains. Eur J Biochem 269:3779–3788

Wong-Staal F, Chanda PK, Ghrayeb JH (1987) Human immunodeficiency virus: the eighth gene. AIDS Res Hum Retroviruses 3:33–39

Woolley GA, Wallace BA (1992) Model ion channels: gramicidin and alamethicin. J Membr Biol 129:109–136

Yang L, Harroun TA, Weiss TM, Ding L, Huang HW (2001) Barrel-stave model or toroidal model? A case study on melittin pores. Biophys J 81:1475–1485